

# **BJET**

# (Bayero Journal of Engineering and Technology)

https://bjet.ng/index.php/jet

# INFLUENCE OF Sb<sub>2</sub>O<sub>3</sub> NANOPARTICLES ON THE PHYSICAL AND MECHANICAL PROPERTIES OF BIOGENIC RICE HUSK SILICATE BOROCALCIUM GLASS FOR PHOTOVOLTAIC APPLICATIONS

# H.S. Ibrahim<sup>1,2,</sup> M. S. Umar<sup>2</sup>, I. O. Oluwansanmi<sup>3</sup>

<sup>1</sup>Directorate of Engineering Infrastructure, National Agency for Science and Engineering Infrastructure (NASENI), Abuja, Nigeria 
<sup>2</sup>Department of Mechanical Engineering, Nigerian Defense Academy (NDA), Kaduna, Nigeria 
<sup>3</sup>Physics Department, Nigerian Defense Academy (NDA), Kaduna, Nigeria

Email: ishassan11@gmail.com

Received: 16-06-2025 Revised: 08-07-2025 Accepted: 13-07-2025 Published: 14-07-2025 **Abstract** Biogenic glass materials, synthesized from agricultural waste, present a sustainable pathway for photovoltaic glass applications. However, the enhancement of these materials through nanoparticle incorporation, specifically to improve physical and mechanical properties, has not been extensively studied. This study investigates the influence of Sb<sub>2</sub>O<sub>3</sub> nanoparticles on the physical and mechanical properties of borocalcium silicate glass, which is derived from high-purity rice husk silica and eggshell calcium oxide. Six glass compositions, with Sb<sub>2</sub>O<sub>3</sub> nanoparticle contents ranging from 0 to 25 wt%, were fabricated using a melt-quenching technique. The density, Vickers microhardness, and indentation fracture toughness of these compositions were then evaluated. The results demonstrated a progressive increase in density (2.518 to 2.939 g/cm³) and microhardness (638 to 875 kgf/mm²), along with enhanced fracture toughness (2.0 to 3.9 MPa·m¹ ²²). These improvements confirm enhanced atomic packing and structural reinforcement, attributed to the Sb<sub>2</sub>O<sub>3</sub> NPs, which promote cross-linking and suppress flaw development. The enhanced mechanical performance and structural integrity of the Sb<sub>2</sub>O<sub>3</sub>-doped biogenic glass establish its viability for PV module encapsulation in mechanically demanding environments.

**Key words**: photovoltaic glass; Rice husk SiO<sub>2</sub>; Eggshell Cao; Nanoparticles; Melt-quench technique; Silicate Borocalcium glass

#### 1 Introduction

Glass materials are indispensable in various advanced industrial sectors, notably electronics and photovoltaic (PV) systems, owing to their unique combination of transparency, chemical stability, and mechanical robustness (Axinte, 2011). Silicate glasses function as dielectric substrates and encapsulants, ensuring structural and electrical integrity under demanding operational conditions (Katti and Sharma, 2023). In photovoltaic modules, the front-surface cover glass is essential for high optical transmittance and resistance to mechanical impacts and thermal cycling, protecting against cell damage and efficiency degradation (Chowdhury *et al.*, 2025;Nayshevsky *et al.*, 2020);Lisco *et al.*, 2020). The increasing frequency of

extreme weather events, such as heavy hailstorms and strong winds, further underscores the critical need for enhanced mechanical resistance in PV panels, often outweighing pure energy efficiency. Traditional glass production, however, is resource-intensive, leading to significant environmental consequences. This has driven current research towards sustainable synthesis methods utilizing alternative raw materials from agricultural and bio-waste streams (Olorunshogo, et al., 2024). Rice husk ash (RHA) and eggshell-derived calcium oxide (CaO) are promising sustainable resources, with RHA containing over 95% amorphous SiO<sub>2</sub> exhibiting melt-quenching behavior suitable for producing high-quality glass (Halimah et al., 2019;Umar et al., 2019;Gonçalves et 2020);Palakurthy et al., 2020) and eggshell CaO

enhancing network connectivity and mechanical robustness as a network modifier (Yamin *et al.*, 2022). This transition promotes waste valorization and aligns with circular economy goals, reducing dependence on mined resources (Islam *et al.*, 2024). While these biogenic materials offer a sustainable foundation for glass development, a comprehensive exploration of their physical and mechanical properties, particularly when enhanced with nanoparticle incorporation, is paramount to assess their suitability for the rigorous demands of PV applications.

The rigorous conditions under which glasses are employed, particularly in photovoltaic applications, necessitate thorough characterization of their physical and mechanical properties. Density, as a key physical attribute, directly influences the durability and performance of glass (Umar et al., 2020). In addition, Vickers hardness and fracture toughness provide crucial metrics for evaluating the glass's mechanical attributes, such as resistance to surface deformation and susceptibility to crack propagation (Guesmia et al., 2022; Barlet et al., 2015). For physical properties, density measurement via Archimedes' method is explored to provide insights into the structural compactness, atomic packing efficiency, and overall rigidity of the glass network (Osfouri and Simon, 2023). When considering mechanical properties of glass, Vickers microhardness testing, preferred for its precision, reproducibility, and simplicity, effectively characterizes a material's resistance to localized plastic deformation(Gong, Chen and Li, 2001; Subhash, Chandra and Koeppel, 2002)

Previous research has extensively explored the mechanical properties of various glass systems and the influence of dopants and waste-derived materials. For instance, (Karabulut et al., 2001) investigated the mechanical and structural properties of sodium and zinc iron-aluminum-phosphate bulk glass and fibers, finding that zinc-containing fibers exhibited higher tensile strength, though strength decreased upon air exposure. In the realm of biomedical applications,. (Xin et al., 2013) comprehensively evaluated the mechanical properties of strong porous scaffolds of silicate 13-93 bioactive glass, demonstrating their potential for load-bearing bone repair despite initial strength decreases in simulated body fluid. (Zhai et al., 2014), specifically investigated borosilicate foam glasses, reporting that appropriate Sb<sub>2</sub>O<sub>3</sub> doping positively impacted bulk porosity and compressive strength, leading to more uniform microstructure and improved performance. Further studies by (Kilinc and Hand, 2015), examined the effects of varying alkaline earth oxide content in soda-lime-silica glasses, observing that mechanical properties tended to

decrease with increasing network connectivity, and that magnesia and lime had different effects on connectivity. Addressing approaches, (Aktas et al., 2017) explored the use of peanut shell powder as a dopant in soda-lime-silica glasses, finding that its addition increased hardness, Young's modulus, and fracture toughness while decreasing density. Similarly, (Borisade et al., 2024), explored repurposing waste glass into silicate-based bioactive glass-ceramics, noting that mechanical properties like micro-hardness and compressive strength varied with phosphate content, showing promise for biomedical applications. investigations have focused on structural modifications and their impact on mechanical performance; (Baino and Fiume, 2019) investigated the porosity dependence of elastic properties in scaffolds, establishing silicate power-law relationships between porosity and mechanical properties, while (Bruns et al., 2020) showed that Al<sub>2</sub>O<sub>3</sub> addition softened alkali-borosilicate glass and enhanced crack resistance by influencing network interconnectivity. More recently, (Karlsson, 2022) studied TiO2-doped soda lime silicate glass, demonstrating that chemical strengthening significantly increased hardness and crack resistance, with specific compositional factors playing a key role.

Specifically, antimony oxide (Sb<sub>2</sub>O<sub>3</sub>) doping, functioning as both a network former and modifier via Sb<sup>3+</sup>/Sb<sup>5+</sup>, has been shown to positively affect glass structure, density, and mechanical performance by promoting structural cross-linking and enhancing densification in conventional glass compositions (Zhai et al., 2014). Furthermore, Sb<sub>2</sub>O<sub>3</sub> can act as a redox agent, facilitating the production of transparent glass from raw materials containing impurities like manganese (Chen et al., 2020; Gonçalves et al., 2020). Despite these established benefits of Sb<sub>2</sub>O<sub>3</sub> in other glass systems and the growing interest in sustainable materials from agricultural waste, there is a notable gap in research specifically examining the effects of Sb<sub>2</sub>O<sub>3</sub> nanoparticles in biogenic silicate-borocalcium glass systems synthesized from rice husk silica and eggshell CaO, particularly concerning their physical and mechanical properties for demanding PV applications. Existing literature on biogenic glass for PV primarily focuses on sustainability aspects, with limited detailed investigation into advanced mechanical reinforcement strategies using such dopants.

Addressing this significant research gap, this study presents a novel investigation into the systematic effects of Sb<sub>2</sub>O<sub>3</sub> nanoparticles on the properties of biogenic glass. The originality of this work lies in its

focused exploration of the precise influence of Sb<sub>2</sub>O<sub>3</sub> nanoparticles on the physical and mechanical characteristics of rice husk silicate borocalcium glass (RHSBCG). This glass is synthesized entirely from high-purity rice husk silica and eggshell calcium oxide and specifically tailored for photovoltaic applications. The aim is to elucidate how Sb<sub>2</sub>O<sub>3</sub> doping, across varying concentrations, affects the physical and mechanical properties of this sustainable biogenic glass. To achieve this, six glass compositions, with a base mass composition of 50SiO2-15Na2O-10CaO-25B<sub>2</sub>O<sub>3</sub>, were systematically fabricated using a meltquenching technique, incorporating incremental additions of Sb<sub>2</sub>O<sub>3</sub> nanoparticles ranging from 0 to 25 wt%. The objective was to rigorously characterize the resulting materials' density, Vickers microhardness, and indentation fracture toughness. This provides comprehensive insights into their structural compactness, resistance to deformation, and crack propagation behavior, thereby establishing their potential viability for PV module encapsulation in mechanically demanding environments.

#### 2 Materials and Methods

#### 2.1 Materials

The materials utilized in this study comprised both commercially procured and locally sourced components, with their respective purity as itemized in Table 1. Specifically, hydrochloric acid, sodium hydroxide, boric acid, and antimony trioxide nanoparticles were obtained from commercial suppliers. Distilled water was prepared in the laboratory and used throughout all experimental procedures. Moreover, FARO 44 rice husk, sourced from Bagudu Local Government Area of Kebbi State, and eggshells collected from Lafia LGA of Nasarawa State, as shown in Figures 1 and 2, served as primary precursors for the extraction of silica and calcium oxide, respectively.

**Table 1: List of Materials Employed** 

Materials	Source/Supplier	Purity	Batch No
HCL	JHD product	98.8	-
Distiled Water	laboratory	-	-
FARO 44 Rice	Bagudu LGA	-	-
Husk			
$SiO_2$	Extracted	98.89	-
Eggshell	Lafia LGA	-	-
CaO	Extracted	98.58	-
$H_3BO_3$	Molychem	99.5	MCR-
			26042
NaOH	Krmel	98	-
$Sb_2O_3$ NPs	Molychem	98.5	MCR-
	•		26746



Figure 1: Rice Husk



Figure 2: Eggshell

#### 2.2 Methods

#### 2.2.1 Glass Synthesis

Glass synthesis was conducted using a conventional melt-quenching technique. Samples were formulated based on a composition of 50SiO2-15Na2O-10CaO-25B<sub>2</sub>O<sub>3</sub>-<sub>x</sub>Sb<sub>2</sub>O<sub>3</sub>, with x being the Sb<sub>2</sub>O<sub>3</sub> NPs varied from 0 to 25 wt% in 5 wt% increments, resulting in six unique glass compositions. Each 20 g batch was stoichiometrically calculated and precisely weighed using a digital microbalance. Before melting, each composition was thoroughly homogenized via mechanical stirring and preheated in an alumina crucible at 400 °C for 1 hour to eliminate residual moisture( Aliyu et al., 2024). The glass mixtures were then melted in an electric furnace at 1100 °C for 3 hours to ensure complete fusion and homogeneity ( Sadiq et al., 2024). The molten glass was cast into preheated stainless-steel cylindrical molds to minimize thermal shock. The glass was then annealed at 400 °C for 1 hour to relieve internal stresses and enhance structural integrity (Hamza et al., 2019). Following a controlled cooling process to room temperature within the furnace, the glass samples were retrieved prepared subsequent characterization.

# 2.2.2 X-ray fluorescence (XRF)

The Elemental analysis of the extracted silica and calcium oxide was performed using a Spectrometer model ARL QUANT'X EDXRF with serial no

9952120, at the Central Laboratory of Umaru Musa Yar'adua University, Katsina. The powders were loaded into sample cups lined with Prolene film, sealed, and mounted in the Genius IF XRF sample turret. The X-ray lamp was pre-warmed, and voltage and emission current were optimized to maintain a dead time of 35–40% for accurate spectral resolution. Spectral data were acquired and processed with XRS-FP software, employing the Master Oxide.tfr file as a calibration reference to quantify the elemental composition of the silica samples.

#### 2.2.3 Physical Property

The physical characterization of the synthesized glass samples was performed via density determination using an automatic density meter (Model MH-300A, serial no 20230409001-2) at the TetFund Central Laboratory, Federal University of Lafia. Measurements were conducted under standard ambient conditions following Archimedes' principle, with distilled water serving as the immersion medium. The instrument automatically calculated the density of each sample based on the recorded weights in air and submerged in water, employing Archimedes' relation given by Equation 1.

$$\rho_{glass} = \frac{w_{glass}}{w_{glass} - w_{liquid}} \rho_{liquid}$$
 (1)

Where  $w_{glass}$  is the weight of the sample in air,  $w_{liquid}$  is the submerged weight, and  $\rho$  is the density (Tan *et al.*, 2023;Osfouri and Simon, 2023)

#### 2.2.4 Mechanical Property

The mechanical properties of the synthesized glass samples were evaluated by microindentation testing using a Vickers hardness tester (Model MV1-PC, Serial No. 07/2012-1329) at the Shell Office, Ahmadu Bello University, Zaria. Polished glass surfaces were indented with a diamond pyramid indenter under a constant load of 0.3 kgf (2.942 N) and a dwell time of 15 seconds. To account for microstructural heterogeneity, a minimum of five indentations were performed per sample at randomly selected locations. The diagonals of each indentation impression were measured using the tester's integrated optical microscope, and Vickers hardness (Hv) was calculated according to Equation 2

$$Hv = \frac{1.8544P}{d^2} \tag{2}$$

where P is the applied load and d is the average diagonal length (Subhash and Koeppel, 2002; Aktas *et al.*, 2017). Furthermore, fracture toughness (K<sub>IC</sub>) was

determined using the modified Anstis relation in equation 3

$$K_{IC} = 0.016 \left(\frac{E}{H_{\nu}}\right)^{\frac{1}{2}} \left(\frac{P}{G^{\frac{3}{2}}}\right)$$
 (3)

where E is the elastic modulus assumed from literature values for borosilicate glass as E = 10H (Lassnig and Zak, 2023), Hv is Vickers hardness, P is the indentation load, and C is the radial crack length from the indentation center to the crack tip obtained with the aid of the optical microscope. Special care was taken to ensure that cracks were of the radial-median type to validate the application of the Anstis relation (Okamoto et al., 2019). This dual-assessment approach enabled the evaluation of resistance to plastic deformation and crack propagation, providing a comprehensive measure of mechanical durability under localized stress conditions.

# 3 Results and Discussion

### 3.1 Extraction and Compositional Analysis

The compositional analysis of the biogenic materials (Tables 2 and 3) confirms the successful extraction of high-purity precursors, underscoring their applicability in advanced glass systems, particularly for photovoltaic (PV) cover glass. Rice husk-derived silica vielded approximately 20 wt.% relative to the raw biomass and exhibited a brilliant white, granulated powder morphology, indicative of efficient organic matter elimination and particulate refinement, as shown in Figure 3. Elemental analysis revealed a SiO2 content of 98.89 wt.%, affirming the efficacy of the acid leaching and high-temperature thermal treatment in removing residual metallic and carbonaceous impurities. (Nzereogu et al., 2023; Aliyu, et al., 2024). This level of purity is consistent with previous findings by Azat et al., 2019; Ajeel, et al., 2021; Geidam et al., 2022; Aliyu et al., 2024, who reported SiO<sub>2</sub> purities of 99.7%, 96.83%, 98.36%, and 97.2%, respectively, using comparable calcination and purification methodologies. Similarly, the eggshell-derived calcium oxide exhibited a high CaO purity of 98.58 wt.% and appeared as a fine white powder, with a yield of approximately 60 wt.% relative to the raw eggshell, as shown in Figure 4. This high conversion efficiency confirms the complete thermal decomposition of calcium carbonate (CaCO<sub>3</sub>) via controlled calcination, as evidenced by the absence of residual carbonate phases (Rinaudo & Morales, 2024; Zia & Riaz, 2025). These findings are consistent with the report by Chuakham et al., 2025, who documented CaO purities in the range of 96-98%. These high-purity yields not only validate the efficacy of the implemented extraction and purification methodologies but also minimize potential interference from secondary phases during

the glass synthesis. The inherent compositional integrity of these biogenic oxides facilitates their seamless integration into the borocalcium silicate glass matrix, providing reliable network formers and modifiers essential for attaining consistent mechanical and physical properties in photovoltaic glass applications.



Figure 3: Extracted Rice Husk SiO<sub>2</sub>



Figure 4: Extracted Eggshell CaO

Table 2: XRF Analysis of the Extracted Rice Husk Silica

	ASII	
Oxides %		
	Concentration	
	in Silica	
	Powder	
$SiO_2$	98.89	
$V_{2}O_{5}$	0.002	
$Cr_2O_3$	0.007	
MnO	0.033	
$Fe_2O_3$	0.119	
NiO	0.001	
CuO	0.035	
$Nb_2O_5$	0.001	
$P_2O_5$	0.026	
$SO_3$	0.109	
CaO	0.423	
$K_20$	0.057	
BaO	0.001	
$Al_2O_3$	0.204	
Ta <sub>2</sub> O <sub>5</sub>	0.001	
$TiO_2$	0.043	
ZnO	0.005	
$Ag_2O$	0.001	
Čl	0.04	
$ZrO_2$	0.001	
PbO	0.001	

Table 3: XRF Analysis of the Extracted Calcium Oxide

Oxides	%	
	Concentration	
	In CaO	
	powder	
$SiO_2$	0.302	
$V_{2}O_{5}$	0.013	
$Cr_2O_3$	0.001	
MnO	0.003	
$Fe_2O_3$	0.034	
CoO	0.036	
NiO	0.017	
CuO	0.035	
$Nb_2O_5$	0.007	
$WO_3$	0.013	
$P_2O_5$	0.004	
$SO_3$	0.02	
CaO	98.58	
BaO	0.02	
$Al_2O_3$	0.748	
$Ta_2O_5$	0.007	
$TiO_2$	0.036	
ZnO	0.012	
$ZrO_2$	0.037	
SnO <sub>2</sub>	0.075	

# 3.2 Glass Synthesis

A series of borocalcium silicate glasses were synthesized, employing rice husk-derived silica and eggshell-derived CaO, with the addition of Sb<sub>2</sub>O<sub>3</sub> nanoparticles in varying concentrations as shown in Figure 5. Glass 1 served as the undoped control sample, while Glasses 2-6 incorporated progressively increasing Sb<sub>2</sub>O<sub>3</sub> content. While all samples exhibited optical transparency, a progressively deepening yellow tint was observed in the Sb<sub>2</sub>O<sub>3</sub>-doped glasses, ranging from Glass 2 to Glass 6. This coloration can be attributed to strong absorption phenomena in the far-UV region, specifically the spin-forbidden ¹S₀ → <sup>3</sup>P<sub>1</sub> transitions of Sb<sup>3+</sup> and charge-transfer transitions of Sb5+ occurring above 50,000 cm-1 (Som and Karmakar, 2011; Allen et al., 2013; Divya and Abraham, 2020).



Figure 5: Synthesized Glass Sample with Varying Composition of Sb<sub>2</sub>O<sub>3</sub>

# 3.3 Physical Properties

#### **Density**

The density of the synthesized borocalcium silicate glasses, as presented in Figure 6, shows a consistent increase with the progressive incorporation of Sb<sub>2</sub>O<sub>3</sub> nanoparticles. This trend reflects systematic structural densification, indicative of enhanced atomic packing and increased network rigidity. Such behavior aligns with the findings of Allahmoradi and Rajabi 2017, who reported similar densification in antimonycontaining glass systems. The observed increase is primarily attributed to the dual role of Sb<sub>2</sub>O<sub>3</sub>: functioning as a network modifier at lower concentrations and transitioning to a partial network former at higher loadings, thereby reinforcing the glass matrix. (Nalin et al., 2001). Additionally, the increase in density is explained by the partial substitution of lighter constituent atoms within the glass matrix, such as silicon (28.09 g/mol) and boron (10.81 g/mol), with the substantially heavier antimony atoms (121.76 g/mol), thereby contributing to overall mass densification. This substitution not only increases the atomic mass contribution per unit volume but also induces topological modifications in the glass matrix (Alcock, 2001). Specifically, Sb<sup>3+</sup> ions participate in the formation of structural units, integrating into the silicate-borate network, which enhances network connectivity and reduces free volume. Progressively increasing the concentration of Sb<sub>2</sub>O<sub>3</sub> nanoparticles disrupts Si-O-Si and B-O-B linkages, facilitating a rearrangement of the glass structure towards a denser configuration (Wang, and Zhang, 2020). The increased density significantly affects the glass's mechanical and thermal performance (Gayathri et al., 2011). A denser glass network inherently enhances resistance to elastic deformation and suppresses microcrack propagation, as noted by Ali 2022. This attribute is particularly critical for photovoltaic (PV) cover glass, which is frequently exposed to mechanical loading and cyclic thermal stresses. The improvement in fracture resistance is further substantiated by the elevated fracture toughness (K<sub>IC</sub>) values presented in Figure 6. Additionally, the increased network rigidity resulting from Sb<sub>2</sub>O<sub>3</sub> doping contributes to a measurable rise in both the glass transition temperature and softening point, thereby enhancing the thermal stability of the material under extreme operating conditions (Zhai et al., 2014). Collectively, these improvements affirm the functional suitability of the synthesized biogenic glasses for durable and resilient PV module integration, particularly in high-irradiance thermally fluctuating environments.

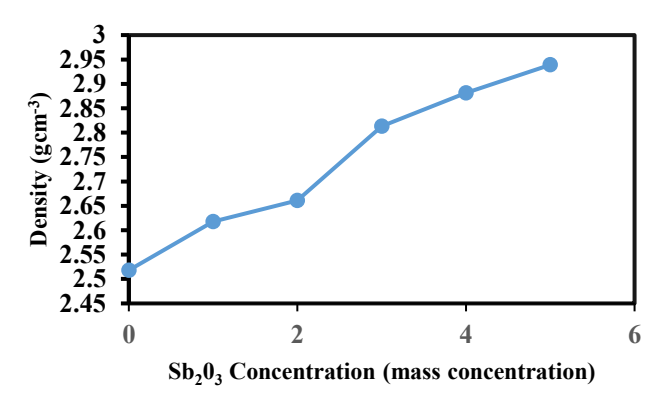


Figure 6: Density of the Synthesized Sb<sub>2</sub>O<sub>3</sub> RHSBCG

# 3.4 **3.4 Mechanical Properties**

# 3.4.1 Hardness and Fracture Toughness

The Vickers microhardness of the synthesized rice husk silica borocalcium glasses, as a function of Sb<sub>2</sub>O<sub>3</sub> concentration, is illustrated in Figure 7. The host glass (GL1) exhibited an initial hardness of 638 kgf/mm<sup>2</sup>. A slight decline to 529.3 kgf/mm<sup>2</sup> was observed in GL2 (5 wt.% Sb<sub>2</sub>O<sub>3</sub>), likely due to initial network disruption. However, with further dopant addition, a steady increase in hardness was recorded, reaching a maximum of 875 kgf/mm<sup>2</sup> in GL6. This trend is consistent with the observations of Barlet et al., 2015; Aktas et al., (2017), who reported enhanced microhardness in doped SLS glass systems. The improvement is attributed to Sb<sub>2</sub>O<sub>3</sub>-induced structural reconfiguration, which enhances resistance to plastic deformation by increasing bond strength and reducing network mobility (Souri & Torkashvand, 2017). The influence of Sb<sub>2</sub>O<sub>3</sub> on the glass network is distinctly concentration dependent. At lower concentrations, Sb<sub>2</sub>O<sub>3</sub> appears to function primarily as a network modifier by introducing non-bridging oxygen sites, which can locally weaken the glass network and account for the initial slight reduction in hardness observed in GL2. However, with increasing concentrations, Sb<sub>2</sub>O<sub>3</sub> transitions to a more prominent network-forming role, participating in structural units that enhance mean bond strength and overall network rigidity. This dual behaviour of antimony in glass systems is documented in the literature, including the work of Allahmoradi and Rajabi (2017), Furthermore, the substitution of lighter cations with heavier Sb atoms contributes to a greater atomic packing density and overall densification (Ali, 2022), which synergistically enhances the material's resistance to indentation. Mechanically, the observed increase in Vickers hardness signifies improved durability and greater resistance to abrasion and mechanical fatigue. These attributes are essential for photovoltaic cover glasses, which are continuously exposed to dynamic environmental stresses and require robust surface integrity for long-term performance.

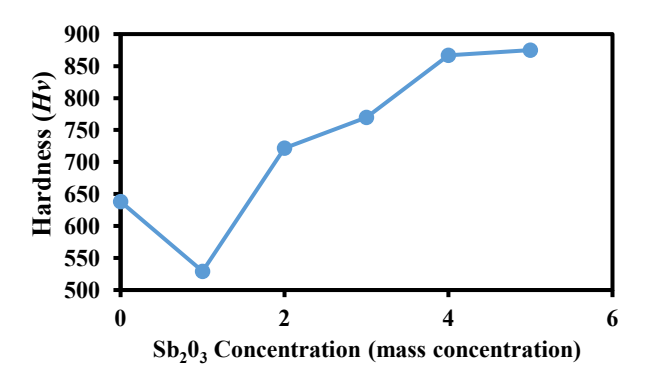


Figure 7: Hardness (Hv) of the Synthesized Sb203-doped RHSBCG

Figure 8 illustrates the relationship between the indentation fracture toughness of the synthesized glass samples and the concentration of Sb<sub>2</sub>O<sub>3</sub> nanoparticles. The host glass exhibited an initial toughness of approximately 0.67 MPa·m<sup>1/2</sup>, which showed a steady increase with the incorporation of Sb<sub>2</sub>O<sub>3</sub>, reaching values between 0.8-0.99 MPa·m<sup>1/2</sup> for samples containing 20-25 wt% Sb<sub>2</sub>O<sub>3</sub>. The enhanced fracture toughness can be attributed to several structural mechanisms. Elevated Sb<sub>2</sub>O<sub>3</sub> concentrations promote the formation of isotropic Sb-O-Sb linkages and network densification (Zhai et al., 2014), thereby augmenting the glass's capacity for energy dissipation under mechanical stress. Additionally, the potential development of residual compressive stresses resulting from thermal expansion mismatch between Sb-rich and Si-rich domains may impede crack propagation, further improving fracture resistance. These observations are consistent with similar findings, which demonstrated increased fracture toughness in soda-lime-silica glasses; they attributed this improvement to enhanced Si-O-Si network polymerization and bond stabilization (Hand and Tadjiev, 2010). While increased network connectivity typically diminishes glass ductility, the Sb<sub>2</sub>O<sub>3</sub>-doped systems investigated herein sustain a beneficial equilibrium between stiffness and compliance. Notably, this trend aligns with the findings of Humood, Beheshti, and Polycarpou 2017, who reported that glasses with elevated fracture toughness values demonstrate significantly susceptibility to flaw-induced catastrophic failure, thereby ensuring more reliable long-term mechanical performance in photovoltaic modules. The fracture toughness of glass is intrinsically dependent on crack

geometry, as described by the standard Vickers indentation relation. In the GL4 sample, the observation of unusually long radial cracks, despite the material's high hardness, resulted in a lower-than-expected K<sub>IC</sub> value. This outcome highlights the significant influence of crack length and elastic-plastic mismatch, where increased stiffness, without effective crack arrest mechanisms, leads to diminished toughness. A similar trend was reported by Sayyed et al., 2021, in which Sb<sub>2</sub>O<sub>3</sub>-doped soda-lime glass exhibited increased hardness but decreased fracture toughness due to enhanced crack propagation.

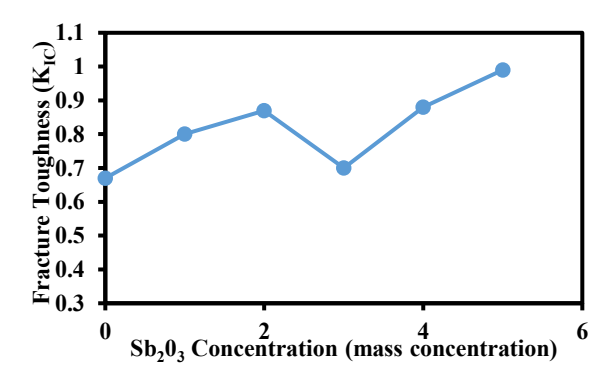


Figure 8: Fracture Toughness  $K_{IC}$  of the Synthesized  $Sb_2\theta_3$ -doped RHSBCG

The concurrent improvement in hardness and fracture resistance confirms the structural reinforcement imparted by the Sb<sub>2</sub>O<sub>3</sub> NPs additive. This reinforces the suitability of the glass as a durable, mechanically resilient PV glass, capable of withstanding both mechanical load and environmental degradation. These results demonstrate the mechanical reliability of the developed bio-derived glass for high-performance photovoltaic applications in regions like Nigeria, where thermal and mechanical stability are essential.

#### 4 Conclusion

This study successfully investigated the impact of Sb<sub>2</sub>O<sub>3</sub> nanoparticles on the physical and mechanical properties of biogenic rice husk silicate borocalcium glass (RHSBCG) developed for photovoltaic applications. High-purity SiO<sub>2</sub> and CaO, derived from rice husk and eggshells, were incorporated into a borocalcium silicate matrix utilizing a melt-quenching method. Archimedes' principle and Vickers microhardness testing were employed to determine the physical and mechanical properties. The incremental addition of Sb<sub>2</sub>O<sub>3</sub> resulted in a significant increase in density, Vickers microhardness, and indentation fracture toughness, indicating enhanced atomic packing, surface hardness, and resistance to crack

propagation. These improvements are attributed to the structural role of Sb<sub>2</sub>O<sub>3</sub>, which functions as a network modifier at low concentrations and a network former at higher concentrations. The results confirm the mechanical viability of the synthesized biogenic glass for durable and sustainable PV cover systems. Consequently, further research should assess the longterm environmental stability of the doped glass under realistic PV operating conditions, considering UV radiation, thermal cycling, and mechanical abrasion. Furthermore, optical, and spectral conversion analyses are recommended to evaluate the influence of Sb<sub>2</sub>O<sub>3</sub> on light management and the overall performance of solar modules. The incorporation of this bio-derived, antimony-enhanced glass presents a promising avenue for developing environmentally sustainable and structurally robust photovoltaic technologies.

# Acknowledgement

We gratefully acknowledge the Nigerian Defense Academy (NDA), Kaduna, and the Department of Mechanical Engineering for providing institutional support throughout the course of this research.

#### References

- Aktas, B. *et al.* (2017) 'Mechanical properties of soda-limesilica glasses with variable peanut shell contents', *Acta Physica Polonica A*, 131(3), pp. 511–513. https://doi.org/10.12693/APhysPolA.131.511.
- Alcock, C.B. (2001) 'Physical and chemical properties of glassy and liquid silicates', in *Thermochemical Processes*. Elsevier, pp. 307–316. https://doi.org/10.1016/B978-075065155-4/50014-1.
- Ali, S. (2022) 'Impact of the Atomic Packing

  Density on the Properties of Nitrogen-Rich Calcium
  Silicate Oxynitride Glasses', *Materials*, 15(17).

  https://doi.org/10.3390/ma15176054.
- Aliyu, S. et al., (2024) 'Bismuthite and cassiterite-doped borosilicate glass systems for X-rays attenuation: Fabrication and characterisation', Optical Materials, 151 p. 115365. https://doi.org/10.1016/j.optmat.2024.115365.
- Aliyu, A. et al.. (2024) 'Optoelectronic and gamma ray attenuation properties of ore-based Bi and Sn-doped borosilicate glasses', Ceramics International, 50(15), pp. 26424–26434.https://doi.org/10.1016/j.ceramint.2024.04.36
- Aliyu, S. et al., (2024) 'Synthesis and characterisation of rice husk and palm fruit bunch silica: compositional, structural, and thermal analyses', Biomass Conversion and Biorefinery [https://doi.org/10.1007/s13399-024-05525-1.
- Allahmoradi, N., Baghshahi, S. and Rajabi, M. (2017) 'The role of Sb2O3 on the physical and structural properties of PbO-SiO2 glasses', *Journal of Ceramic Processing Research*, 18(9), pp. 691–695.
- Allen, J.P. et al. (2013) 'Electronic structures

- of antimony oxides', *Journal of Physical Chemistry C*, 117(28), pp. 14759–14769. https://doi.org/10.1021/jp4026249.
- Axinte, E. (2011) 'Glasses as engineering materials: A review', *Materials and Design*, 32(4), pp. 1717–1732. https://doi.org/10.1016/j.matdes.2010.11.057
- Baino, F. and Fiume, E. (2019) 'Elastic mechanical properties of 45S5-based bioactive glass-ceramic scaffolds', *Materials*, 12(19). https://doi.org/10.3390/ma12193244.
- Barlet, M. et al. (2015) 'Hardness and toughness of sodium borosilicate glasses via Vickers's indentations', Journal of Non-Crystalline Solids, 417–418, pp. 66–79. https://doi.org/10.1016/j.jnoncrysol.2015.02.005.
- Borisade, S.G. *et al.* (2024) 'Investigation of physical, mechanical and in-vitro bioactivity of bioactive glass-ceramics fabricated from waste sodalime-silica glass doped P2O5 by microwave irradiation sintering', *Hybrid Advances*, 6, p. 100203.

  Available at: https://doi.org/10.1016/j.hybadv.2024.100203.
- Bruns, S. et al. (2020) 'Influence of Al2O3
  Addition on Structure and Mechanical Properties of Borosilicate Glasses', Frontiers in Materials, 7.: https://doi.org/10.3389/fmats.2020.00189.
- Chen, T.Y. et al. (2020) 'Compositionstructure-property effects of antimony in soda-limesilica glasses', Journal of Non-Crystalline Solids, 544.
  - https://doi.org/10.1016/j.jnoncrysol.2020.120184.
- Chowdhury, T. et al. (2025) 'Review of issues and opportunities for glass supply for photovoltaic production at multiterawatt (TW) scale', Sustainable Energy and Fuels, pp. 1414–1431. https://doi.org/10.1039/d4se01567c.
- Chuakham, S. et al. (2025) 'Scalable production of bio-calcium oxide via thermal decomposition of solid hatchery waste in a laboratory-scale rotary kiln', Scientific Reports, 15(1), pp. 1–15. https://doi.org/10.1038/s41598-024-84889-w.
- Divya, K. V. and Abraham, K.E. (2020) 'Ag nanoparticle decorated Sb2O3thin film: synthesis, characterizations and application', *Nano Express*, 1(2), p. 20005. https://doi.org/10.1088/2632-959X/aba103.
- Gayathri Pavani, P., Sadhana, K. and Chandra Mouli, V. (2011) 'Optical, physical and structural studies of boro-zinc tellurite glasses', *Physica B: Condensed Matter*, 406(6–7), pp. 1242–1247. https://doi.org/10.1016/j.physb.2011.01.006.
- Gonçalves, J. et al. (2020) 'Production of transparent soda-lime glass from rice husk containing iron and manganese impurities', Ceramics, 3(4), pp. 494–506.https://doi.org/10.3390/ceramics3040040.
- Gong, J., Chen, Y. and Li, C. (2001) 'Statistical analysis of fracture toughness of soda-lime glass determined by indentation', *Journal of Non-Crystalline Solids*, 279(2–3), pp. 219–223. https://doi.org/10.1016/S0022-3093(00)00418-X.
- Guesmia, N. et al. (2022) 'Glass formation, physical and structural investigation studies of the (90-x) Sb2O3-10WO3-xNaPO3 glasses', Materials Today Communications, 30, p. 103226.

- https://doi.org/10.1016/j.mtcomm.2022.103226.
- Halimah, M.K. *et al.* (2019) 'Study of rice husk silicate effects on the elastic, physical and structural properties of borotellurite glasses', *Materials Chemistry and Physics*, 238(July), p. 121891. https://doi.org/10.1016/j.matchemphys.2019.121891
- Hamza, A.M. *et al.* (2019) 'Structural, optical and thermal properties of Er3+-Ag codoped biosilicate borotellurite glass', *Results in Physics*, 14(March), p. 102457.https://doi.org/10.1016/j.rinp.2019.102457.
- Hand, R.J. and Tadjiev, D.R. (2010)

  'Mechanical properties of silicate glasses as a function of composition', *Journal of Non-Crystalline Solids*, 356(44–49), pp. 2417–2423. https://doi.org/10.1016/j.jnoncrysol.2010.05.007.
- Humood, M., Beheshti, A. and Polycarpou, A.A. (2017) 'Surface reliability of annealed and tempered solar protective glasses: Indentation and scratch behavior', *Solar Energy*, 142, pp. 13– 25.https://doi.org/10.1016/j.solener.2016.12.011.
- Islam, M.T. et al. (2024) 'Production and
  Characterization of Silica from Rice Husk: An
  Updated Review', Asian Journal of Chemical
  Sciences, 14(2), pp. 83–96.
  https://doi.org/10.9734/ajocs/2024/v14i2296.
  Karabulut, M. et al. (2001) 'Mechanical and
  structural properties of phosphate glasses', Journal of
  Non-Crystalline Solids, 288(1–3), pp. 8–17.
  https://doi.org/10.1016/S0022-3093(01)00615-9.
- Karlsson, S. (2022) 'Compositional Effects on Indentation Mechanical Properties of Chemically Strengthened TiO2-Doped Soda Lime Silicate Glasses', *Materials*, 15(2).https://doi.org/10.3390/ma15020577.
- Katti, A. and Sharma, Y. (2023) Photonic

  Materials: Recent Advances and Emerging
  Applications, Photonic Materials. Pune: World
  Peace University Pune India.
  https://doi.org/10.2174/97898150497561230101.
- Kilinc, E. and Hand, R.J. (2015) 'Mechanical properties of soda-lime-silica glasses with varying alkaline earth contents', *Journal of Non-Crystalline Solids*, 429, pp. 190–197. https://doi.org/10.1016/j.jnoncrysol.2015.08.013.
- Lassnig, A. and Zak, S. (2023) 'Precise determination of Young's modulus of amorphous CuZr/nanocrystalline Cu multilayer via nanoindentation', *Journal of Materials Research*, 38(13), pp. 3324–3335. https://doi.org/10.1557/s43578-023-01057-y.
- Lisco, F. *et al.* (2020) 'Degradation of Hydrophobic, Anti-Soiling Coatings for Solar Module Cover Glass', *energies*, 13(3811), pp. 1–15.
- Nalin, M. *et al.* (2001) 'Antimony oxide based glasses', *Journal of Non-Crystalline Solids*, 284(1–3), pp. 110–116. https://doi.org/10.1016/S0022-3093(01)00388-X.
- Nayshevsky, I. et al. (2020) 'Fluoropolymer coatings for solar cover glass: Anti-soiling mechanisms in the presence of dew', Solar Energy Materials and Solar Cells, 206, p. 110281. https://doi.org/10.1016/j.solmat.2019.110281.
- Nzereogu, P.U. *et al.* (2023) 'Silica extraction from rice husk: Comprehensive review and

- applications', *Hybrid Advances*, 4, p.100111.https://doi.org/10.1016/j.hybadv.2023.100 111.
- Okamoto, T. et al. (2019) 'The structure and properties of xZnO–(67–x)SnO–33P 2 O 5 glasses: (IV) Mechanical properties', Journal of Non-Crystalline Solids, 513(February), pp. 44–48. https://doi.org/10.1016/j.jnoncrysol.2019.02.030.
- Olorunshogo, B.O., Azubuike Chukwudi
  Okwandu and Sanni, A.A. (2024) 'Recent advances
  in solar photovoltaic technologies: Efficiency,
  materials, and applications', GSC Advanced
  Research and Reviews, 20(1), pp. 159–175.
  https://doi.org/10.30574/gscarr.2024.20.1.0259.
- Osfouri, M. and Simon, A. (2023) 'The detection of porous media volume using the modified Archimedes method', *Epitoanyag Journal of Silicate Based and Composite Materials*, 75(2), pp. 48–51. https://doi.org/10.14382/epitoanyagisbcm.2023.07.
- Palakurthy, S. et al. (2020) 'A cost effective SiO2–CaO–Na2O bio-glass derived from bio-waste resources for biomedical applications', *Progress in Biomaterials*, 9(4), pp. 239–248. https://doi.org/10.1007/s40204-020-00145-0.
- Rinaudo, M.G., Collins, S.E. and Morales,
  M.R. (2024) 'Eggshell Waste Valorization into CaO/CaCO3 Solid Base Catalysts', p. 36. https://doi.org/10.3390/engproc2024067036.
- Sayyed, M.I. et al. (2021) 'Enhancement of the shielding capability of soda–lime glasses with Sb2O3 dopant: A potential material for radiation safety in nuclear installations', Applied Sciences (Switzerland), 11(1), pp. 1–15. https://doi.org/10.3390/app11010326.
- Som, T. and Karmakar, B. (2011)

  'Nephelauxetic effect of low phonon antimony oxide glass in absorption and photoluminescence of rareearth ions', Spectrochimica Acta Part A: Molecular and Biomolecular Spectroscopy, 79(5), pp. 1766–1782. https://doi.org/10.1016/j.saa.2011.05.054.
- Souri, D. and Torkashvand, Z. (2017)

  'Thermomechanical Properties of Sb2O3-TeO2-V2O5 Glassy Systems: Thermal Stability, Glass Forming Tendency and Vickers Hardness', *Journal of Electronic Materials*, 46(4), pp. 2158–2163. https://doi.org/10.1007/s11664-016-5151-8.
- Subhash, G., Chandra, A. and Koeppel, B.J.
  (2002) Apparatus and method for determining the dynamic indentation
- Tan, A.R. *et al.* (2023) 'Graph theory-based structural analysis on density anomaly of silica glass', *Computational Materials Science*, 225, p. 112190. Available at: https://doi.org/10.1016/j.commatsci.2023.112190.
- Umar, S.A. et al. (2019) 'Optical and structural properties of rice husk silicate incorporated borotellurite glasses doped with erbium oxide nanoparticles', Journal of Materials Science: Materials in Electronics, 30(20), pp. 18606–18616.: https://doi.org/10.1007/s10854-019-02213-z.
- Umar, S.A. *et al.* (2020) 'Structural, elastic and thermo-physical properties of Er2O3 nanoparticles doped bio-silicate borotellurite glasses', *SN Applied Sciences*, 2(2), pp. 1–10. Available at: https://doi.org/10.1007/s42452-020-2112-x.

- Wang, Z., Zhao, Y. and Zhang, C. (2020)
  - 'Comparative investigation on the structure and physical properties of CeO2/TiO2/Sb2O3-doped bismuth borosilicate glasses', *Journal of Non-Crystalline Solids*, 544, p. 120190. https://doi.org/10.1016/j.jnoncrysol.2020.120190.
- Xin Liua, Mohamed N. Rahamana, Gregory
  Hilmasa, and S.B. (2013) 'Mechanical properties of
  bioactive glass (13-93) scaffolds fabricated by
  robotic deposition for structural bone repair Xin',
  National Institutue of Health, 61(1), pp. 1–7.
  https://doi.org/10.1016/j.actbio.2013.02.026.Mecha
  nical.
- Yamin, N.A.M. *et al.* (2022) 'Effect of calcium oxide in the zinc-boro-soda-lime-silica glass matrix

- by using eggshell waste as calcium source', *Applied Physics A*, 128(1), p. 93. https://doi.org/10.1007/s00339-021-05241-x.
- Zhai, C. et al. (2014) 'Effects of Sb2O3 on the mechanical properties of the borosilicate foam glasses sintered at low temperature', Advances in Materials Science and Engineering, 2014.https://doi.org/10.1155/2014/703194.
- Zia, J., Shringi, A.K. and Riaz, U. (2025)

  'Calcium oxide nanoparticles from eggshell waste: A green nanotechnological strategy for microwave-assisted environmental clean up', Cleaner Chemical Engineering, 11(May), p. 100182. https://doi.org/10.1016/j.clce.2025.100182.